stresses during gaps closing, which eventually may lead to premature buckling of the steel bars, a steel tube (with an outside diameter of 27 mm and a thickness of 3 mm) was located over the fused length of the damper. In addition, the steel tube was filled with non-shrinking grout. This grouted steel tube system is intended to delay buckling of the fused length, allowing the dampers to yield under tension and compression, even at large walls' drifts. The external dampers were attached to the specimens via strong steel connectors (Fig. 2.b), which were designed to allow quick installation and replacement of the dampers. The steel connectors were fixed to the wall panel by high-strength bolts that passed through the panel section. which were post-tensioned so to avoid any slippage.

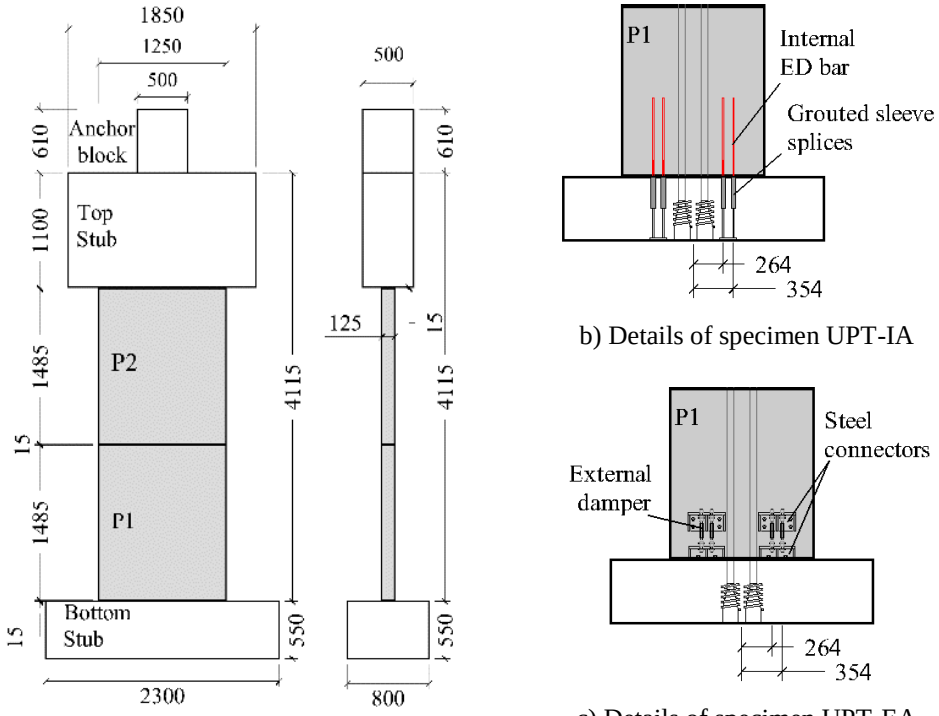

a) Dimensions (units: mm)

b) Details of specimen UPT-IA

c) Details of specimen UPT-EA

Fig. 1 – Details of test specimens

Table 1 shows the measured properties of the concrete used for the panels. The specified concrete strength for all precast units was 60 MPa; however, the measured values of f'_c for precast panels were above 80 MPa. The measured compressive strength of concrete for stubs was about 91 MPa, and the compressive strength of the joint mortar was 102 MPa. Moreover, the measured compressive strength of the dampers grout was 69.4 MPa.

Table 2 presents the average values of the reinforcing bars' material properties. The yielding strength of panel reinforcement and hoops was 403.7 and 889.0 MPa, respectively. Note that high-strength hoops were used to improve the efficiency of confinement and to reduce the required volumetric ratio at the boundary elements. The internal ED bars had a yielding strength of 387.0 MPa, whereas the external hysteretic dampers showed a yielding strength of about 360.8 MPa. As for the PT reinforcement material properties, two types of strands were used and the measured values of tensile strength (f_{pu}) were 1992.7 and 1910.3 MPa for the epoxy-coated and uncoated strands, respectively; moreover, the measured values of yielding strength (f_{py}), calculated as the 0.2% offset stress, was 1824.5 and 1803.6 MPa for the coated and uncoated strands, respectively.

3. Test setup

The loading setup for the experiment can be seen in Fig. 3. Horizontal loads were applied by a servo-controlled, 3000 kN-capacity hydraulic jack, which was attached to the specimen top stub by a rigid steel jig. The lateral loads were applied at a level of 3265 mm from the bottom joint. The vertical load was applied by two 1000 kN vertical jacks. A total axial load of 468.5 kN (which represents an axial load ratio of 0.05) was applied to the specimen, prior to any lateral load application, and kept constant throughout the test. After the axial load was applied, displacement-controlled, fully reversed cyclic loads were applied to the specimen with peak drifts of 1/6000, 1/800, 1/400, 1/200, 1/100, 1/50, 1/33, 1/25 and 1/20 rad. Two full cycles were applied at each peak drift, except for 1/6000 drift where only one cycle was applied. The loading was stopped when a strength degradation of above 20% of the maximum lateral load was observed or after a drift of 5%.

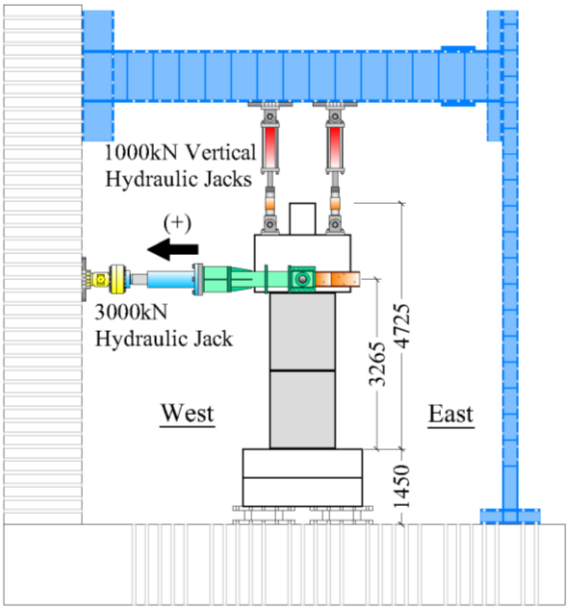

Fig. 3 – Details of test specimens

4. Test results

Fig. 4 shows the measured base shear force-drift behavior of the specimens, with the observed limit states also indicated. Despite the total axial load ratio, due to gravity loads, vertical loads, and prestressing force, being considerable (0.07 for UPT-IA and 0.08 for UPT-EA), both specimens sustained drifts larger than 3% without significant strength degradation and with minor damage. The peak shear force was 301 and 320 kN at -3% drift for UPT-IA and UPT-EA, respectively. After achieving the peak shear force, strength degradation was observed due to the fracture of either internal ED bars or external dampers.

Fig. 5 shows the final condition of the specimens. Damage in the specimens was limited to the base panel and no damage was observed on the upper panel. Gap opening became visible from 0.125% drifts as a crack at the base joint for both specimens. Moreover, minor flexural cracks started to appear on the surface of the base panel at 0.25% drift for both specimens, but they fully closed when the specimens were unloaded. Cover concrete spalling was initially observed at drifts of 1% in both specimens, and by the end of the test, cover concrete spalling was limited to a relatively small area at the toes of the wall (about 400 mm long and 150 mm high for UPT-IA). Nevertheless, it was observed that the core concrete and confinement hoops were sound after the test, making the boundary elements still able to sustain the axial load. Moreover, the crushing of the base joint mortar was observed after 3% drifts.

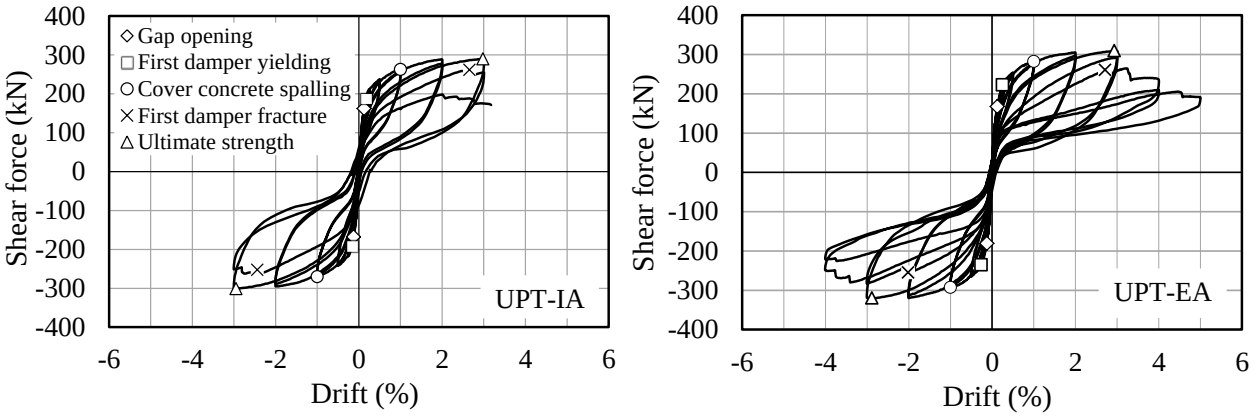

Fig. 4 – Load-Deformation behavior of test specimens

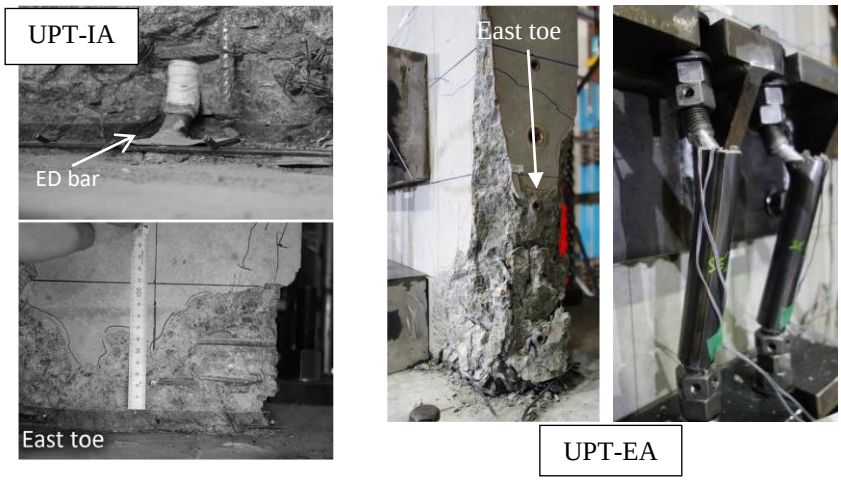

Fig. 5 – Final condition of specimens

The yielding of ED bars and external dampers provided the main source of energy dissipation in their corresponding specimen. The ED bars of specimen UPT-IA started to yield at 0.17% drift, whereas external dampers started to yield at 0.25% drift on UPT-EA. Buckling of the unbonded length of ED bars was noted at large drifts, 2nd cycle at 3%, prior to fracturing, which pushed the surrounding concrete outward and caused unexpected cover concrete spalling at the center of the base panel (See Fig. 2). This buckling of ED bars also caused an out-of-plane displacement (to the north) of UPT-IA, which reached a large as 20 mm by the end of the test. One of the ED bars (at the east side) fractured first during the 2nd cycle of the 3% drift in UPT-IA and was followed by three more bars, which fractured on the way to the next peak drift of the 4% drift. This fracture of the ED bars caused a strength degradation of more than 30% of the peak load and resulted at the end of the test. The significant buckling can be considered as the reason for the earlier fracture of ED bars compared to the external dampers, and the out-of-plane displacement, in addition to the earlier fracture of dampers, is attributed as the main cause for the significant strength degradation in specimen UPT-IA.

Despite using steel tubes, the external dampers also suffer from localized flexural buckling, at the top end (see Fig.5), before fracturing. However, all the dampers fractured under tensile stresses, after providing considerable energy dissipation. Moreover, the external dampers could be replaced after the test. The first external damper, at the east side of UPT-EA, fractured during the 1st cycle of the 4% drift and was immediately followed by two more dampers, which fracture in the same cycle, causing a strength degradation below 30%. After this, one more loading cycle, until 5% peak drift, caused the fracture of the last damper on the east side of UPT-EA. After the test, all the fractured dampers could be removed easily,

which allows a quick replacement, if necessary, and validates the design of the damper and connector configurations.

Fig. 6 shows the measured PT tendon stresses. The PT tendons provided the main restoring force to the specimens and it was observed that they remained within the elastic range (yielding strength was 1803MPa) throughout the test. There was some loss in the PT force, which can be attributed to the strand-anchorage interaction and the damage of the bottom joint mortar. The maximum prestress loss was about 10% for UPT-IA and 20% for UPT-EA of the initial prestressing force. It has been reported that certain PT anchorages may cause the premature fracture of PT strands when they are subjected to cyclic inelastic stresses [4,5]. In this test, the PT anchorages performed adequately, preventing premature fracture of tendons, mainly because the stresses in the tendons were below the yield strength, as it was designed.

The measured values of relative energy dissipation ratio are shown in Fig. 7. The relative energy dissipation ratio β, as defined in the ACI ITG-5.2 [6], was used to quantify the amount of energy dissipation of the specimens. It is required that β should be no less than 0.125 at the maximum strength level so to ensure [6]. It was observed that both ED bars and external dampers provided an adequate amount of energy dissipation to the specimens until their peak strength was reached. UPT-IA showed larger β than UPT-EA, which can be attributed to the larger contribution of the cover concrete due to the ED bar buckling. Nonetheless, the use of external dampers in UPT-EA resulted in less concrete spalling and provided a quick replacement of dampers after the test, which is critical to restoring the capacity on UPT walls after a severe earthquake.

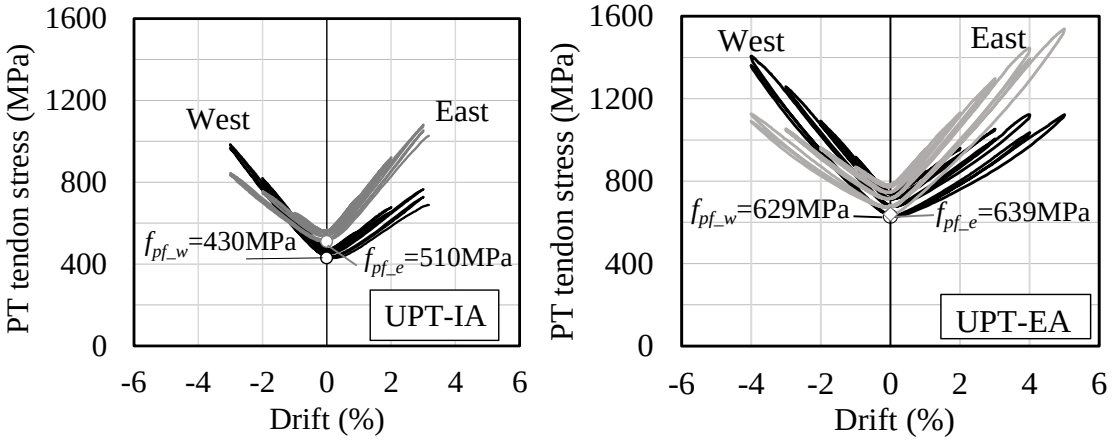

Fig. 6 – Stresses variation in PT tendons

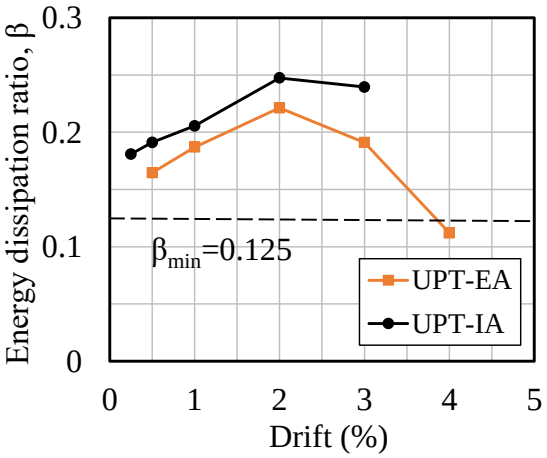

Fig. 7 – Values of relative energy dissipation ratio

